J Seismol (2008) 12:323–341
DOI 10.1007/s10950-008-9094-2

REVIEW

Probabilistic seismic hazard assessment of the Pyrenean region

R. Secanell · D. Bertil · C. Martin · X. Goula · T. Susagna · M. Tapia · P. Dominique · D. Carbon · J. Fleta

Received: 15 February 2006 / Accepted: 4 February 2008 / Published online: 25 March 2008

Abstract A unified probabilistic seismic hazard assessment (PSHA) for the Pyrenean region has been performed by an international team composed of experts from Spain and France during the Interreg IIIA ISARD project. It is motivated by incoherencies between the seismic hazard zonations of the design codes of France and Spain and by the need for input data to be used to define earthquake scenarios. A great effort was invested in the homogenisation of the input data. All existing seismic data are collected in a database and lead to a unified catalogue using a local magnitude scale. PSHA has been performed using logic trees combined with Monte Carlo simulations to account for both epistemic and aleatory uncertainties. As an alternative to hazard calculation based on seismic sources zone models, a zoneless method is also used to produce a hazard map less dependant on zone boundaries. Two seismogenic source models were defined to take into account the different interpretations existing among specialists. A new regional ground-motion prediction equation based on regional data has been proposed. It was used in combination with published ground-motion prediction equations derived using European and Mediterranean data. The application of this methodology leads to the definition of seismic hazard maps for 475- and 1,975-year return periods for spectral accelerations at periods of 0 (corresponding to peak ground acceleration), 0.1, 0.3, 0.6, 1 and 2 s. Median and percentiles 15% and 85% acceleration contour lines are represented. Finally, the seismic catalogue is used to produce a map of the maximum acceleration expected for comparison with the probabilistic hazard maps. The hazard maps are produced using a grid of 0.1°. The results obtained may be useful for civil protection and risk prevention purposes in France, Spain and Andorra.

Keywords Seismic hazard · Monte Carlo · Probabilistic · Seismic zonation · France · Spain · Andorra

R. Secanell · C. Martin · D. Carbon
GEOTER, Pòle Géoenvironment,
3, rue Jean Monnet,
24830 Clapiers, France
e-mail: ramon.secanell@geoter.fr

X. Goula · T. Susagna (✉) · M. Tapia · J. Fleta
Institut Geològic de Catalunya (IGC),
Balmes, 209–211,
08006 Barcelona, Spain
e-mail: tsusagna@icc.es

D. Bertil · P. Dominique
Bureau de Recherches Géologiques et Minières (BRGM),
3, Avenue Claude Guillemin,
45060 Orléans Cedex 2, France

M. Tapia
Centre Mediterrani d'Investigacions Marines
i Ambientals (CSIC-CMIMA),
passeig Marítim de la Barceloneta, 37-49,
08003 Barcelona, Spain

1 Introduction

For regions situated at the border of two countries, seismic hazard assessments made by different teams can show significant differences, particularly in low-seismicity areas where input data are poorly constrained. The Pyrenees on the France–Spain border are especially concerned by this problem. For example, peak ground acceleration (PGA) proposed for a 475-year return period in the present Spanish building code (NCSE-02 2002) for this area ranges from 0.04 to 0.12*g*. In a recent probabilistic study for its use in a seismic zonation of France, Martin et al. (2002a) found PGA levels varying from 0.15 to 0.25*g* for the same region and return period. With another probabilistic methodology, Marin et al. (2004) report a maximum PGA of 0.067*g*. The Global Seismic Hazard Assessment Project gives an equivalent maximum PGA in the western French Pyrenees of 0.17*g* and in Spanish Catalonia 0.18*g* (Jiménez et al. 1999). This kind of heterogeneity of hazard maps can be explained by differences in methodology, seismogenic zonation, seismicity catalogues and by uncertainties in the data interpretations.

One of the objectives of the Interreg IIIA ISARD project, carried out by an international team composed of experts from Spain and France, was to reduce these observed incoherencies and provide homogeneous seismic hazard estimates at the border of the two countries. This article presents the probabilistic seismic hazard assessment (PSHA) carried out during this project.

In accordance with the international practice of seismic hazard evaluation (e.g. Abrahamson 2000), PSHA must take into account both epistemic and aleatory uncertainties associated to input parameters. Epistemic uncertainty refers to insufficient knowledge. It cannot be measured and is evaluated by expert judgement. The most widely used tool for handling epistemic uncertainty in PSHA is the logic tree. Aleatory uncertainties include the inherent randomness in the characterization of seismic source parameters and attenuation relations.

In the logic tree proposed for this study, epistemic uncertainties relate to the conceptual model of seismic hazard assessment, different seismogenic zonations, identification of the most applicable ground-motion prediction equations and choice of the conversion formulae between different magnitude definitions. Aleatory uncertainties include annual activity rate and *b* value distributions, focal depth and maximum magnitude distributions inside source zones. Impacts on hazard assessment of the aleatory uncertainties of input data are evaluated with a Monte Carlo approach.

In a first step, all available historical and instrumental seismic data from French and Spanish catalogues are collected and compared to build a single homogeneous catalogue usable for PSHA.

Results are represented as two seismic hazard maps for 475- and 1,975-year return periods.

2 Geological and tectonic setting

The Pyrenees are a 400-km-long mountain range located in southwest Europe along the French–Spanish border. Geological and geophysical studies (e.g. the Etude Continentale et Oceanique par Reflexion et Refraction Sismique seismic profile, Daignières et al. 1989) show a crustal thickening under an axial zone associated with a partial subduction of the Iberian Plate beneath the European plate. Apart from this axial zone, an asymmetric doubly vergent structure with North and South major thrust faults is associated with two foreland basins: the Ebro basin to the south and the Aquitanian basin to the north.

Geodynamic evolution of the mountain belt is dominated initially by strike–slip movement (107 to 90 Ma) and then by convergence (90 to 20 Ma) between the Iberian and Eurasian plates (Olivet 1996). From the Oligo-Aquitanian to the Burdigalian period (34 to 20 Ma), the eastern part of the Pyrenees was affected by the extension phase associated with the opening of the Gulf of Lion passive margin and with the southeastward drifting of the Corsica–Sardinia block. The tectonic regime gradually changed from extension to compression due to the North–South convergence between African and European plates (Goula et al. 1999). The Neogene and Quaternary evolution of Pyrenees (since 20 Ma) indicates a relatively slow convergence (Verges 1993). Alasset and Meghraoui (2005) assume that the deformation rate through Pyrenees during the Quaternary is less than 1 mm/year. Current deformations are monitored by repetitive global positioning system measurements since 1992 (Talaya et al. 1999). However, measurements show non-significant tectonic deformation rates that are lower than the uncertainties (0.5±1.5 mm/year; Nocquet 2002).

3 ISARD seismic catalogue

Seismic data corresponding to a region limited by latitudes 40°–44° N and longitudes 2.5° W–4° E for seismic events until 2003 were collected. The ISARD catalogue is built by merging historical and instrumental data. Macroseismic and instrumental data are first treated separately. Afterwards, the two sources of information are merged.

3.1 Macroseismic and instrumental input data

Four macroseismic catalogues have been analysed: the catalogue of the Servei Geològic de Catalunya – SGC (Susagna and Goula 1999), the catalogue of the Instituto Geográfico Nacional – IGN (Mezcua and Martinez-Solares 1983) updated by Martinez-Solares and Mezcua (2002), the Sisfrance catalogue (BRGM et al. 2004) and the Levret et al. (1996) catalogue analysing 140 well-documented historical earthquakes.

The intensity scale is the Medvedev–Sponheuer–Karnik (MSK) except for IGN, which has updated the MSK to the European macroseismic scale for data up until 1900 (Martinez-Solares and Mezcua 2002). A window in latitude, longitude and epicentral intensity is used to identify earthquakes reported by several catalogues. Manual revision is performed to verify and correct possible errors in the automatic process. Only one reference is kept for date, time and epicentral coordinates with priority for Sisfrance data and then SGC data. The epicentral intensity retained is an average of available values from the different catalogues.

Five instrumental catalogues have been consulted covering different areas and time intervals. The oldest ones are provided by, for France, the Laboratoire de Détection Géophysique (LDG) starting in 1962 and, for Spain, by the IGN-I since 1961. Regional catalogues are more recent: since 1977 for SGC (2003) and since 1989 for the catalogue of Observatoire Midi Pyrénées – OMP (Souriau and Pauchet 1998). The French national instrumental catalogue provided by the Bureau Central Sismologique Français (BCSF) starts in 1980. The M_L local magnitude is the magnitude scale generally used by the different catalogues. IGN use the $m_{b,Lg}$ scale, but for regional distances (less than 1,000 km), this corresponds almost to the same seismic phases as the M_L scale. For that reason, no distinction is made here between $m_{b,Lg}$ and M_L. As for macroseismic catalogues, only one reference is kept for date, time and epicentral coordinates using the following priority of agencies: SGC-I, LDG, IGN-I, BCSF and OMP. M_L magnitude is an average of all available M_L estimates. Table 1 gives an example of earthquake reported by the five agencies.

3.2 ISARD-unified catalogue

The complete ISARD catalogue was compiled by merging the macroseismic and instrumental catalogues described above. From 1961 to 2003, for the earthquakes registered in both catalogues, we adopt the instrumental location and origin time because of the higher precision of instrumental measurements and will keep both magnitude and epicentral intensity information.

Epicentral intensity and magnitude have been assessed by averaging all the available values, whereas time and space parameters are selected from the most reliable sources. With this conceptual choice, internal coherence between epicentral location and source parameters (magnitude or intensity) is not necessarily respected. This subjective choice has been made by the expert team to retain information from all the agencies that have detected the same event and to limit possible over- or under-estimation of magnitude or intensity by an agency by averaging all available information.

Table 1 Example of a earthquake (ID 1221) referenced in the five instrumental catalogues showing the structure of the database

Number	Agency	Longitude	Latitude	Year	Month	Day	Hour	Minute	Second	M_{sgc}	M_{ldg}	M_{omp}	M_{ign}	M_{bcsf}	M_s	M_w	$M_{L\text{-}ISARD}$
1221	OMP	2.53	42.80	1996	2	18	1	45	45.6			5.2					
1221	BCSF	2.50	42.75	1996	2	18	1	45	45.9					5.6			
1221	LDG	2.53	42.83	1996	2	18	1	45	46.0		5.6						
1221	SGC-I	2.54	42.79	1996	2	18	1	45	45.5	5.2							
1221	IGN-I	2.60	42.82	1996	2	18	1	45	45.6				5.0				
1221	ISARD	2.54	42.79	1996	2	18	1	45	45.6								5.3

The magnitude scale adopted in the ISARD catalogue is the local magnitude, M_L. There is not enough data to develop a specific relation between M_L and M_w or M_S for the Pyrenean region. For the instrumental period between 1961 and 2003, only four earthquakes have reported magnitude greater than 5.0 (events in 1961, 1967, 1980, 1996), with a maximum of M_L 5.3. The 1980 event is the only one having an M_w estimate in the Harvard centroid moment tensor catalogue.

For earthquakes with both intensity and magnitude information, a relation between epicentral intensity and local magnitude has been fitted using a least-square regression (Fig. 1). With essentially low magnitude and intensity data, the correlation coefficient is low. However, to verify coherency of this conversion formula with instrumental data, an adjustment of the Gutenberg–Richter (GR) relation has been made using macroseismic and instrument data separately (Fig. 2). The two GR best fittings are in good agreement. For magnitudes greater than 5, macroseismic best fittings give a slightly higher annual earthquake rate, but this is coherent with the GR relation for the global ISARD catalogue.

Sensitivity analysis shows that the fitting is strongly dependant on the choice of the sample data. Other kinds of relationship better fit the few points with intensity larger than V but give a frequency relation that is not coherent with that obtained from the instrumental data. This would mean that the regional seismicity is not stationary and depends on the period of time considered (historic or instrumental). Our intensity–magnitude conversion relation, although poorly constrained, provides the best consistency between macroseismic and instrumental data.

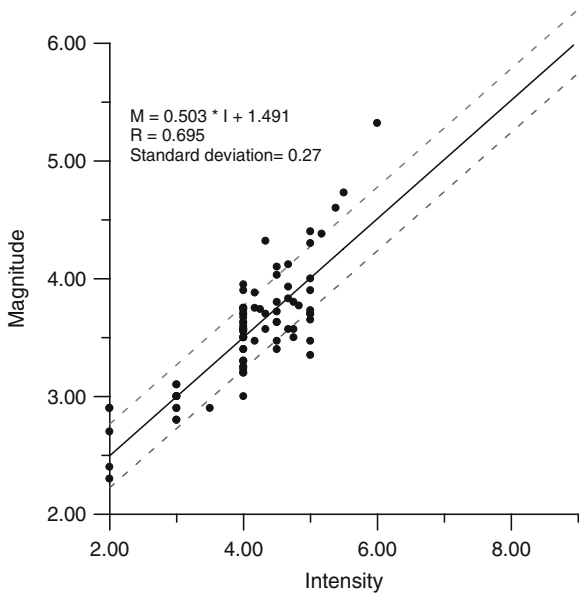

Fig. 1 Magnitude–epicentral intensity linear regression

To satisfy the spatial and temporal principle of independence of the earthquakes, the aftershocks in the catalogue were removed. The process used consisted of the definition of a temporal and spatial window adapted to each range of magnitude (the larger the main shock the larger the temporal and spatial window). All earthquakes situated inside the window defined following a main shock were considered as aftershocks and removed from the catalogue used for PSHA purposes. The temporal and spatial windows used for the determination of aftershocks are presented in Table 2.

Testing of the temporal completeness of the catalogue was performed using the Stepp (1972) methodology and a software package developed by Martin et al. (2002b). The beginnings of the periods of completeness are given in Table 3 and Fig. 3. Large regional earthquakes (M_L>6.0) are assumed to be registered since the beginning of the historical period. Historical records increased gradually since 1750, the beginning of completeness for M_L>5. Data with M_L less than 4.0 are complete only for the instrumental period since 1965. Since then, the progressive increase in seismic stations in the Pyrenean area leads to a gradual reduction in the magnitude threshold with time from 3.9 in 1965 to 2.5 in 1980.

The magnitude and time characteristics are displayed in Fig. 4. The ISARD catalogue lists 1991 events from 1427 to 2003. As Fig. 5 shows, the distribution of earthquakes in the Pyrenees is not homogeneous. The main activity is located to the north of the axial zone, in the central western part of the Pyrenees. This activity seems to be regular with time. More than 20 historical earthquakes with epicentral intensities equal or greater than VII (M5.0) and four with epicentral intensity equal or larger than VIII (M5.5) are reported. In the region of Pamplona, in the Spanish western part of the mountains, the instrumental data show the existence of a cluster of seismicity with two earthquakes with a local magnitude larger than 4.5.

The eastern part of the Pyrenees shows a weaker and diffuse seismicity level both in the number of

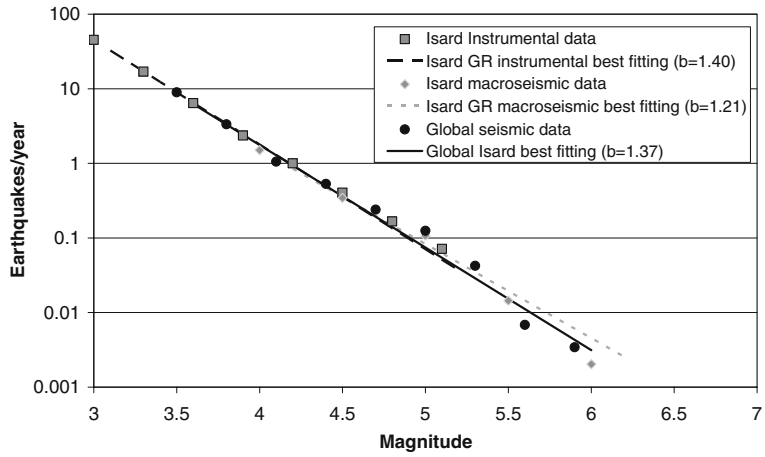

Fig. 2 Comparison of GR relations deduced from macroseismic data and instrumental data

earthquakes and magnitude. However, the historical data are marked by the presence of an important seismic crisis during the fifteenth century, with an epicentral intensity IX (M6.0) for the 1428 event.

Finally, in the region of Barcelona, the seismic activity is characterised by some historical earthquakes with a maximum epicentral intensity equal to VIII (M5.5) during the fifteenth century.

The ISARD catalogue is published on the website of the ISARD project: www.isard.project.eu.

4 Probabilistic assessment

A logic tree is usually defined to take into account the uncertainties associated with fundamental hypotheses related to probabilistic hazard calculations. Each hypothesis is represented by a node on the logic tree. The different proposed alternatives are defined with branches opened at each node. The degree of confidence of each choice is represented by relative weights assigned to the branch.

Table 2 Magnitude and temporal windows used to identify aftershocks

Magnitude (M_L)	Temporal window (month)	Spatial window (km)
4.0–4.9	1	5
5.0–5.4	2	10
5.4–5.9	3	15
6.0–6.5	4	20

The logic tree model developed for this study is illustrated in Fig. 6. The four nodes on the left-hand side represent alternative hypotheses associated with epistemic uncertainties that will be described in detail below. The node on the right-hand side represents aleatory uncertainties associated with seismic source input parameters. Monte Carlo simulations are used to propagate these aleatory uncertainties into the PSHA. The Monte Carlo technique generates a great number of random values of source zone parameters. The number of iterations must be large enough to have a good representation of the probability distribution associated with each parameter. From stability tests and sensitivity analysis, 100 random models were generated for each main branch of the logic tree.

The choice of hypotheses being integrated in the global model were defined by the group of French and Spanish experts involved in the project. To evaluate the branch weights, a table was prepared where each expert indicated their individual opinion

Table 3 Completeness date used for the best fittings of the GR relations

Magnitude (M_L)	Initial date
3.0–3.2	1977
3.3	1970
3.4–3.9	1965
4.0–4.5	1880
4.6–4.9	1830
5.0–5.4	1750
5.5–5.9	1420
6.0–6.5	1000

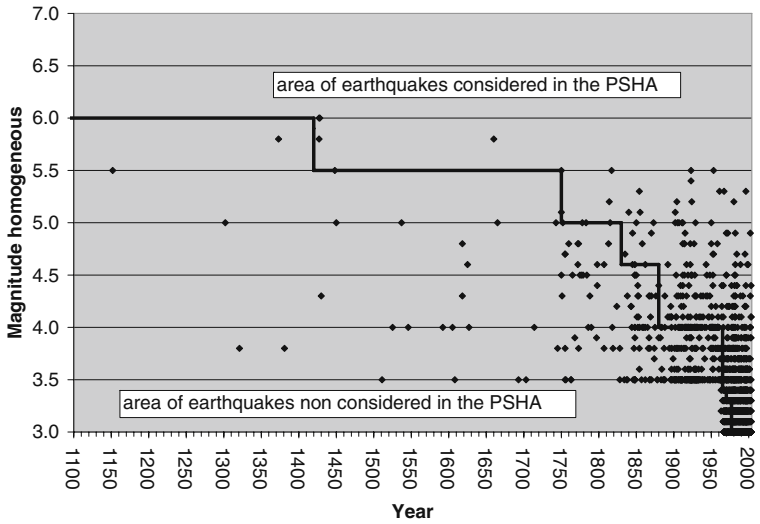

Fig. 3 Stepp-plot analysis of the ISARD catalogue

about the weight of each branch. The final weight adopted (Fig. 6) corresponds to the average of the opinions of all involved experts in the project.

Finally, the logic tree leads to eight independent basic hypotheses to calculate PSHA, and for each of them, the Monte Carlo simulation generates 100 different sequences of source zone parameters. PSHA is calculated for 475- and 1,975-year return periods, for PGA and spectral accelerations (SAs) at periods 0.1, 0.3, 0.6, 1 and 2 s. The median, 15th percentile and 85th percentile values were estimated from statistical processing of the results obtained with this logic tree combined with the Monte Carlo approach.

4.1 Conceptual models

The probabilistic seismic hazard is calculated using the classic methodology originally developed by Cornell (1968) and McGuire (1976). From seismic activity and tectonic behavior, a seismic zonation is proposed with area or fault sources. Inside these zones, seismicity is assumed to be uniform and defined by a small numbers of parameters (activity rate, *b* value, depth and maximum magnitude). However the delimitation and the parametric characterisation of these seismic sources introduce numerous uncertainties in the seismic hazard evaluation. An alternative non-zoning method is developed to reduce the influence of the zone boundaries in the hazard assessment. The methodology is that of Woo (1996), and it is described below. In the logic tree, weights for the zoning and non-zoning models are 0.57 and 0.43, respectively.

4.1.1 Zoning methodology

For this conceptual model, computation is performed using the program CRISIS99 (Ordaz et al. 1999). This software has been largely tested and used in European projects such as RISK-UE (Faccioli 2006) and for the French seismic zonation (Martin et al. 2002a). CRISIS99 is able to include the uncertainty associated with the ground-motion prediction equation, as is standard for PSHA software.

4.1.2 Smoothing methodology

This approach was developed by Woo (1996), and it has been widely used and tested (e.g. for the French zonation, Martin et al. 2002a). The only input data needed for this procedure is a seismic catalogue and ground-motion model. Events outside periods of completeness have already been eliminated from the catalogue.

The method is based on the observation that the distribution of epicentres generally does not satisfy the condition of the uniform distribution assumed by zoning methods. The epicentre of each earthquake able to contribute to the hazard ($M \geq 4.0$) is used to generate a spatial distribution of earthquake occurrence at each point of a user-defined rectangular grid.

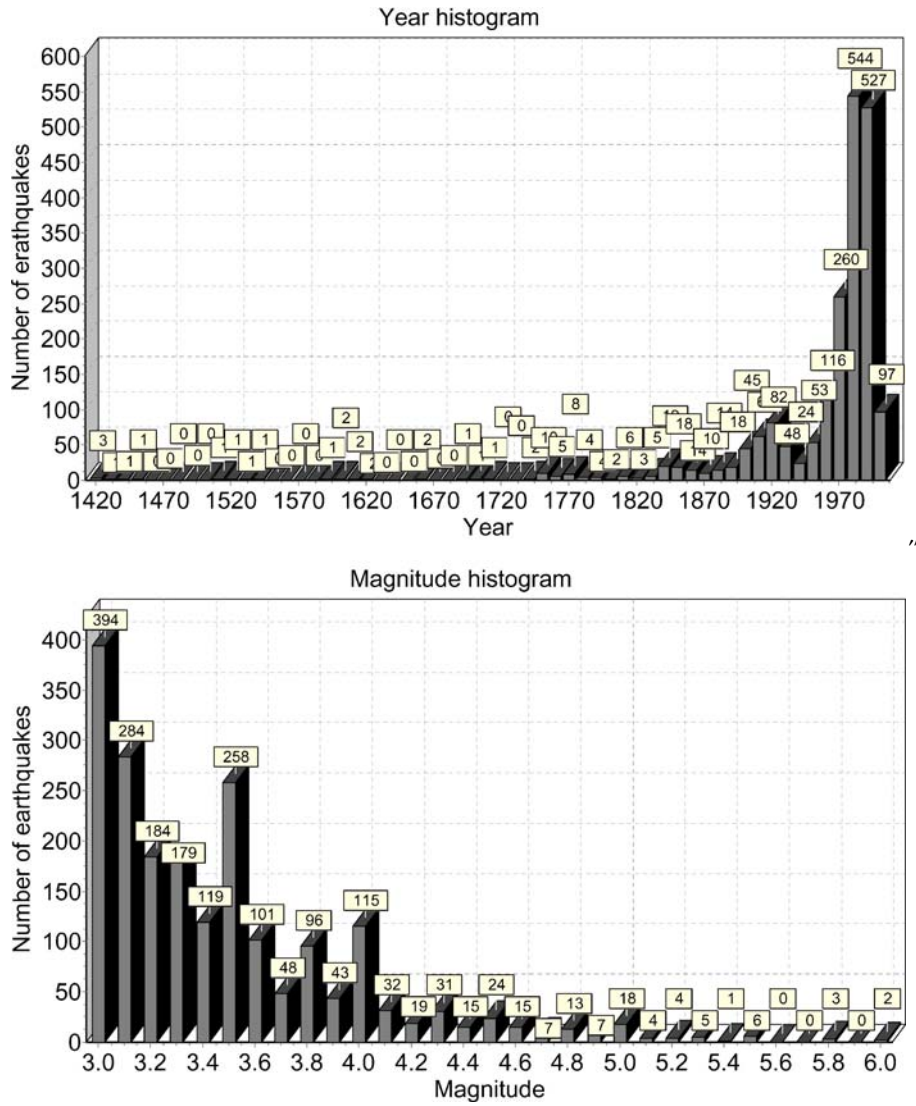

Fig. 4 Time–magnitude histogram of the ISARD catalogue

The size of the grid depends on the resolution desired. In our case, the selected resolution is 0.1°. This approach is consistent with the observation that future earthquakes often occur in the same geographical area as previous past earthquakes. A spatial-smoothing finite kernel function is used to calculate the distribution of magnitudes taking into account the epicentres. For magnitudes between 4.0 and the maximum magnitude defined, $\lambda(M)$, the exceedance rate for magnitude M is calculated at each point of the grid. After that, the method calculates the seismic hazard in a similar way to the zoning procedure.

The kernel function is defined with two spatial parameters R_{min} and R_{max}. R_{min} is fixed to 10 km. R_{max} is assumed to follow a uniform probability distribution between 40 and 60 km. The focal depth, h, of the seismic source is fixed at each point of the grid. Aleatory uncertainties in relation with R_{max} and focal depth are treated with Monte Carlo simulations, as for seismic zoning parameters.

This smoothing method only takes into consideration the information that is registered in the earthquake catalogue, and it is not possible to introduce information about earthquakes with return periods greater than the length of the earthquake database. With the ISARD catalogue, this method gives more importance to the macroseismic data than does the zoning procedure.

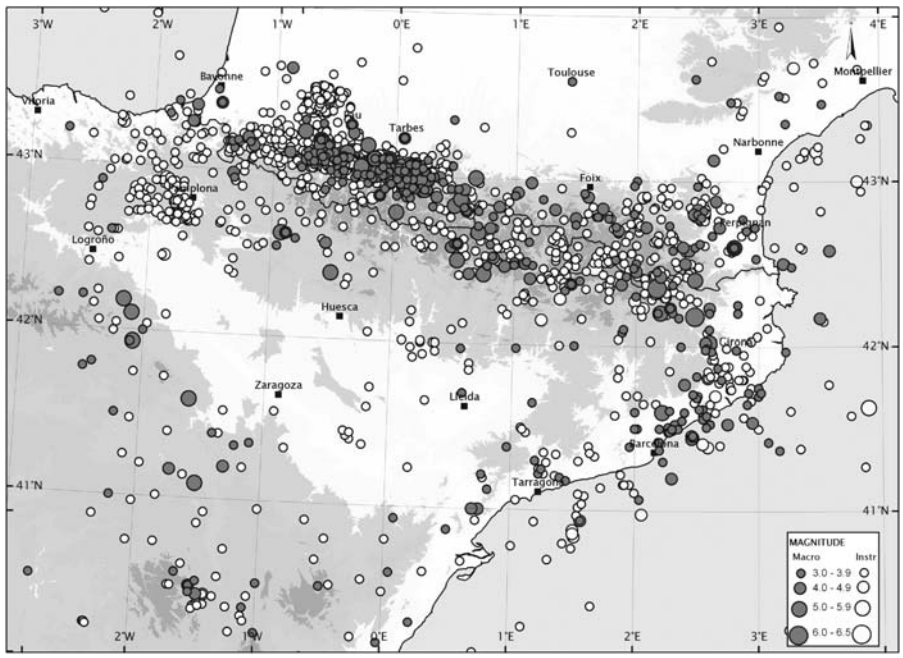

Fig. 5 Historical and instrumental seismicity of Pyrenees from the ISARD catalogue. Epicentral intensities are converted to local magnitude using the relation displayed in Fig. 1

4.2 Seismotectonic models

In a context of moderate seismic activity, there is a lack of knowledge about parameters characterising seismicity related to known active faults. Associated uncertainties are too high to propose a PSHA based on a fault sources model; therefore, only area zones are used in the zonation.

4.2.1 Source zone geometry

Two seismogenic zonations are proposed. The first one is a consensus among different international experts and, for that reason, is called the "unified" seismogenic zonation (USZ). It corresponds to the synthesis of recent studies: Fleta et al. (1996), Secanell et al. (1999), Secanell et al. (2002) and Secanell et al. (2004) for northeastern Spain

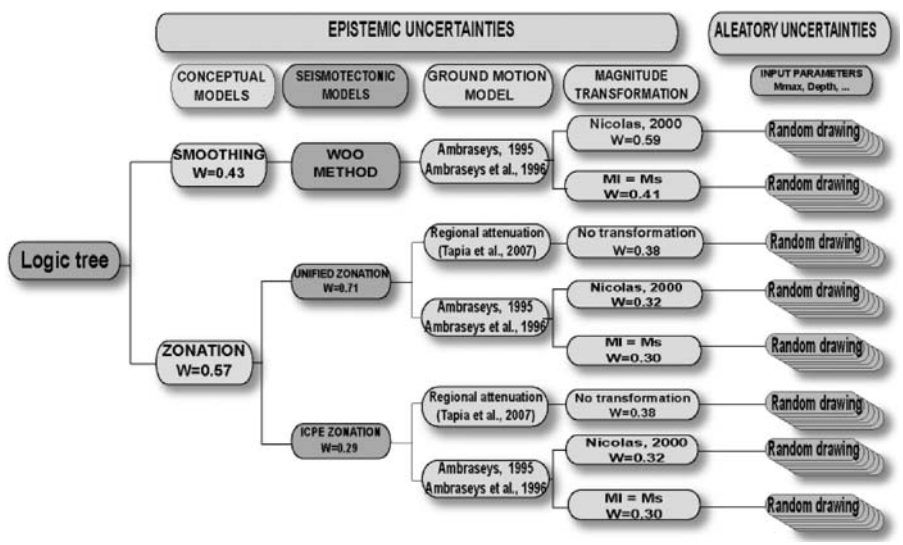

Fig. 6 Logic tree associated with the PSHA methodology

and southwestern France, Autran et al. (1998) and Dominique et al. (1998) for the seismogenic zonation defined by the French working group 'Evaluation Probabiliste de l'Aléa Sismique' of the Association Française du génie Parasismique, and Martin et al. (2002a) for the revised French seismic zonation. USZ is composed of 18 area zones and is illustrated in Fig. 7.

The second one, called the critical facilities zonation (CFZ), is shown in Fig. 8. It is adapted from the seismogenic zonation of Metropolitan France carried out to facilitate and standardize the application of earthquake-resistant building regulations for critical facilities (Blès et al. 1998; Terrier et al. 2000). Twelve of the original zones covering the Pyrenean region in France and a part of Spain north of latitude 42° N are preserved. This zonation model is completed with 11 supplementary zones adapted from the USZ model to cover all the region of this study. Their boundaries are modified to deal with the critical facilities zones selected.

Along the France–Spain border, zone boundaries are very different between the two models. CFZ zones are more aligned with the massif axis. In the UFZ, the zones in Catalonia are more in line with other Mediterranean zones.

The USZ model has well-defined source area limits separating regions with different seismogenic behaviour and results from a consensus of expert judgements. For those reasons, its weight in the logic tree is high (0.71) compared with CFZ (0.29).

4.2.2 Source zone activity parameters

Seismic parameters for the USZ are shown in Table 4 and for CFZ in Table 5. The seismic occurrence model adopted corresponds to the GR double-truncated distribution. For each zone, the double-truncated GR frequency–magnitude distribution is derived from the ISARD catalogue according to the Weichert (1980) method. Activity rates and b values are evaluated using maximum-likelihood estimation for different time periods. This method is well adapted to zones where the completeness period is different for each range of magnitude. GR best fittings are made mainly due to the minimum magnitude M_L 3.0 considered in the ISARD catalogue. Annual activity rate λ is adjusted for the minimum magnitude M_L 4.0 for use in the PSHA. Zones with too few data are grouped together to obtain a global adjustment. Then, λ is recalculated for each zone as a function of its surface area. Regrouped zones are indicated by stars in Tables 4 and 5.

The central western Pyrenean part of the massif is the most active zone (zone 7 in the USZ, Table 4, and zone 3 in CFZ, Table 5). This region is characterized by a high b value (1.3–1.4) and focal depths deeper than for other regions. The occurrence rate of an earthquake with M_L>4.0 is roughly one every 2 years. On the southern zones of each model, annual activity rates are low (the occurrence period of a magnitude 4.0 for the Barcelona region is roughly 15 years), and b values are around 0.9.

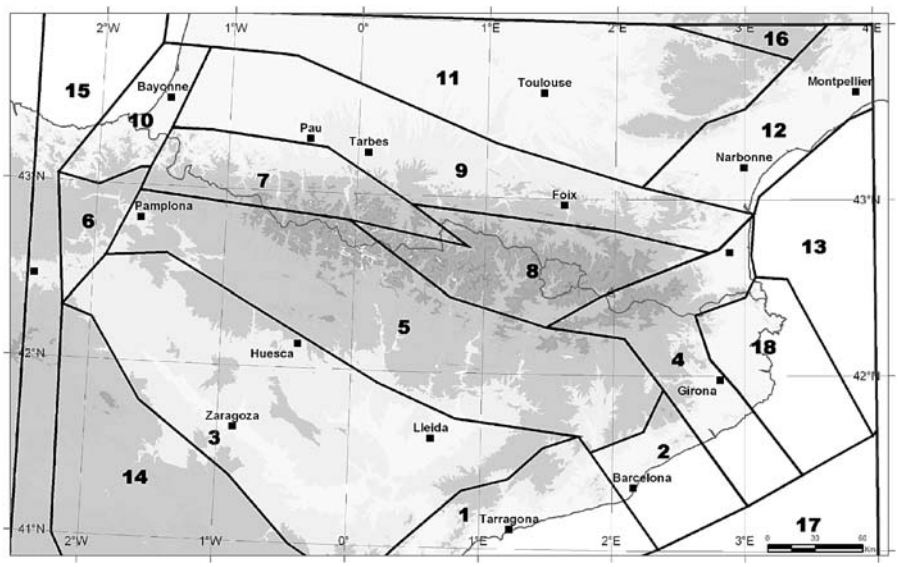

Fig. 7 USZ used for the PSHA

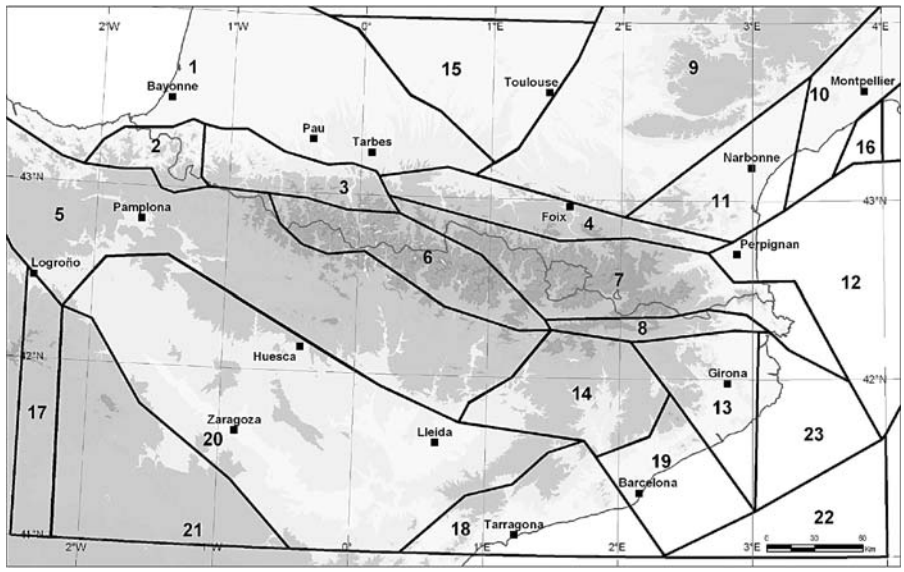

Fig. 8 CFZ used for the PSHA

The depth of each seismic source was fixed following a consensual process between French and Spanish experts. The depth parameter is defined with minimal and maximal bounds rather than by an average value. In most regions, focal depths vary from 5 to 15 km.

The maximum magnitude M_{max} is defined using an arbitrary approach by increasing the maximum ob-

Table 4 Seismic parameters associated with the USZ model

Seismic parameters												
Zone	a	b	σa	σb	λ(M=4)	λ/km^2	β	$\sigma\lambda$	$\sigma\beta$	h (km)	M_{max}	Surface (km^2)
1	2.37	0.91	1.14	0.34	0.056	4.26E−06	2.09	0.045	0.78	5–10	5.4–5.9	13,220
2	3.05	1.06	0.83	0.25	0.064	1.36E−05	2.44	0.040	0.58	5–10	6.0–6.5	4,702
3[a]	2.02	0.92	0.89	0.24	0.021	8.29E−07	2.13	0.019	0.56	5–15	5.0–5.5	25,520
4	3.46	1.08	0.47	0.14	0.131	1.44E−05	2.50	0.036	0.32	5–15	6.3–6.8	9,115
5	4.52	1.37	0.61	0.18	0.111	4.97E−06	3.15	0.028	0.41	5–15	6.3–6.8	22,420
6	2.30	1.04	2.03	0.59	0.014	5.69E−06	2.39	0.014	1.36	5–15	5.1–5.6	2,523
7	4.97	1.27	0.36	0.10	0.784	1.17E−04	2.92	0.062	0.22	10–20	6.3–6.8	6,696
8	3.71	1.13	0.88	0.24	0.147	1.79E−05	2.61	0.065	0.54	5–15	6.0–6.5	8,247
9	3.14	0.99	1.03	0.26	0.145	9.23E−06	2.29	0.085	0.61	5–15	5.8–6.3	15,700
10	2.47	1.04	2.03	0.59	0.021	5.69E−06	2.39	0.021	1.36	5–15	5.0–5.5	3,695
11[a]	1.95	0.92	0.89	0.24	0.018	8.29E−07	2.13	0.016	0.56	5–15	5.0–5.5	21,850
12	3.39	1.24	2.78	0.78	0.027	3.34E−06	2.85	0.027	1.79	5–10	5.3–5.8	8,223
13[a]	1.51	0.92	0.89	0.24	0.007	8.29E−07	2.13	0.006	0.56	5–10	5.0–5.5	7,997
14[a]	2.10	0.80	0.61	0.19	0.078	2.65E−06	1.85	0.046	0.43	5–15	6.0–6.5	29,570
15[a]	1.88	0.92	0.89	0.24	0.015	8.29E−07	2.13	0.014	0.56	5–15	5.0–5.5	18,480
16[a]	0.67	0.92	0.89	0.24	0.001	8.29E−07	2.13	0.001	0.56	5–15	5.0–5.5	1,136
17[a]	2.11	0.92	0.89	0.24	0.026	8.29E−07	2.13	0.023	0.56	5–10	5.0–5.5	31,710
18[a]	1.46	0.92	0.89	0.24	0.006	8.29E−07	2.13	0.005	0.56	5–10	5.0–5.5	7,129

Zone seismic activity parameters are expressed in terms of a and b values of the GR relation or λ (annual activity rate for magnitude$\geq$ 4.0) and β (=b ln(10)). Standard deviations associated with each parameter are displayed in the σ columns. λ/km^2 is the annual activity rate density. Focal depth (h) and maximum magnitude (M_{max}) are expressed in terms of interval ranges for the uniform distribution

[a] Zones for which data have been merged to calculate β and λ/km^2

Table 5 Seismic parameters associated with the CFZ model

Seismic parameters												
Zone	*a*	*b*	σa	σb	λ(M=4)	λ/km^2	β	$\sigma\lambda$	$\sigma\beta$	*h* (km)	M_{max}	Surface (km^2)
1	5.13	1.52	0.36	0.09	0.1133	3.57E−06	3.50	0.0090	0.200	5–15	5.0–5.5	31,770
2	4.80	1.64	0.65	0.16	0.0170	8.14E−06	3.78	0.0023	0.374	5–15	5.5–6.0	2,092
3	5.26	1.38	0.18	0.04	0.5336	1.54E−04	3.19	0.0230	0.091	10–20	6.5–7.0	3,470
4	4.00	1.25	0.42	0.10	0.0954	2.30E−05	2.89	0.0110	0.234	5–15	5.3–5.7	4,145
5	5.41	1.60	0.35	0.09	0.1013	4.45E−06	3.69	0.0080	0.199	5–15	5.9–6.4	22,750
6	4.24	1.31	0.37	0.09	0.0973	1.83E−05	3.02	0.0110	0.207	5–15	5.0–5.5	5,305
7	3.77	1.07	0.47	0.11	0.3115	3.35E−05	2.46	0.0240	0.112	5–15	6.0–6.5	9,293
8	4.68	1.64	0.65	0.16	0.0130	8.14E−06	3.78	0.0017	0.374	5–15	6.3–6.8	1,592
9	3.61	1.27	0.50	0.12	0.0344	9.72E−07	2.92	0.0048	0.285	5–15	5.4–5.9	35,370
10[b]	2.91	1.27	0.50	0.12	0.0069	9.72E−07	2.92	0.0010	0.285	5–10	5.0–5.5	7,116
11[b]	2.76	1.27	0.50	0.12	0.0049	9.72E−07	2.92	0.0007	0.285	5–10	5.5–6.0	4,998
12[b]	3.33	1.27	0.50	0.12	0.0180	9.72E−07	2.92	0.0025	0.285	5–10	5.2–5.7	18,470
13	3.13	1.08	0.57	0.14	0.0645	1.44E−05	2.50	0.0170	0.320	5–15	6.3–6.8	4,485
14	4.52	1.37	0.61	0.18	0.0305	4.95E−06	3.15	0.0043	0.410	5–15	6.1–6.6	6,158
15[a]	1.49	0.92	0.96	0.24	0.0064	8.26E−07	2.13	0.0005	0.560	5–15	5.7–6.2	7,751
16[a]	0.45	0.92	0.96	0.24	0.0006	8.26E−07	2.13	0.0001	0.560	5–15	5.2–5.7	719
17[a]	1.17	0.92	0.96	0.24	0.0031	8.26E−07	2.13	0.0003	0.560	5–15	5.5–6.0	3,776
18	2.08	0.91	1.36	0.34	0.0277	4.24E−06	2.09	0.0036	0.780	5–10	5.5–6.0	6,541
19	3.05	1.06	0.83	0.25	0.0640	1.36E−05	2.44	0.0083	0.580	5–10	6.0–6.5	4,702
20[a]	2.00	0.92	0.96	0.24	0.0211	8.26E−07	2.13	0.0017	0.560	5–10	5.5–6.0	25,590
21	1.66	0.80	0.76	0.19	0.0286	2.64E−06	1.85	0.0031	0.320	5–15	6.0–6.5	10,830
22[a]	1.30	0.92	0.96	0.24	0.0042	8.26E−07	2.13	0.0003	0.560	5–10	5.5–6.0	5,105
23[a]	1.30	0.92	0.96	0.24	0.0042	8.26E−07	2.13	0.0003	0.560	5–10	5.5–6.0	5,090

See Table 4 for details

[a,b] Two groups of zones for which data have been merged to calculate β and λ/km^2

served magnitude by 0.5–1.0 units (depending on the source zone).

4.3 Ground-motion prediction equations (attenuation relations)

The ground-motion prediction equation has the most influence on the computed seismic hazard. Predicted acceleration levels can vary by up to 100% or even higher. Therefore, it is standard practice in seismic hazard assessments to make use of more than one model as a way to account for epistemic uncertainty in ground-motion prediction. In our case, two different kinds of relationships have been selected and evaluated for rock sites.

The first one corresponds to well-known ground-motion prediction equations widely used in the European domain and adapted to the Pyrenees seismic context. Ambraseys (1995) and Ambraseys et al. (1996) fit this criterion. Ambraseys (1995) is a relation for PGA based on 830 records of crustal earthquakes from countries of the Mediterranean area and the Middle East. The model of Ambraseys et al. (1996) is for horizontal response SA, and it is based on 422 records of crustal earthquakes from Europe and the Middle East. Its database contains many near-source records mainly from small and moderate earthquakes. Therefore, this ground motion prediction equation is one of the most adapted to the seismic context of the Pyrenees. In Ambraseys (1995), source distance is depth dependant, while in Ambraseys et al. (1996), source depth is not taken into account. In the PSHA, Ambraseys et al. (1996) is used for SA and Ambraseys (1995) for PGA (in the same branch of the logic tree).

The second ground-motion prediction model was developed using western Mediterranean data by Tapia et al. (2004) for PGA and SA (0.1, 0.3, 0.6, 1.0 and 2.0 s) as part of the ISARD project and was updated

by Tapia et al. (2007). The model was obtained through regression analysis of 334 records from 30 earthquakes located in the Pyrenees, Italy, Morocco, the South of France and southern Spain. Magnitudes ranged from M_L 3.8 to 5.2 and epicentral distances from 6 to 542 km. The Pyrenees region is represented by nine events contributing 102 records. The functional form adopted is: $\log_{10} A = C_1 + C_2 M_L + C_3 \log_{10} r + C_4 r \pm \sigma$ where A is the horizontal component of PGA or SA expressed in g, r is the hypocentral distance, M_L is local magnitude, σ is the standard deviation of $\log_{10}(A)$ and C_1, C_2, C_3, C_4 are coefficients determined by regression analyses. Values of these coefficients for a depth of 10 km are displayed in Table 6.

With a set of records from small to moderate earthquakes, the relation has a limited validity domain. For $M_L \geq 6.0$, the Ambraseys (1995) and Ambraseys et al. (1996) ground-motion prediction equations are preferred. In the range $5.0 < M_L < 6.0$, a transition zone was established because of differences between the predictions from the models. Thus, the regional relation developed corresponds to:

- The relation of Tapia et al. (2007), up to M_L 5.0
- The relations of Ambraseys (1995) and Ambraseys et al. (1996) for M6.0 and interpolated curves, for magnitudes between 5.0 and 6.0

This process is shown schematically in Fig. 9, where the behaviour of the predictive curves is different for small magnitudes (regional data) and large magnitudes.

A higher weight has been adopted for Ambraseys (1995) and Ambraseys et al. (1996) than for the regional attenuation relationship (0.62, 0.38 respectively).

Figure 10 compares the accelerations predicted by the Ambraseys et al. (1996) relationship and the regional relationship developed in this study. Figure 10 has been made using the magnitude and distance of the associated equation (i.e. no transformation of magnitude is applied).

4.4 Magnitude transformation

The compiled ISARD catalogue is defined in terms of local magnitude, M_L, as is the Tapia et al. (2007) ground-motion prediction equation. However, the Ambraseys (1995) and Ambraseys et al. (1996) ground-motion prediction equations are defined in terms of surface wave magnitude, M_S. Hence, M_S to M_L conversion must be considered. Some studies have been made on the relation between these magnitudes scales. The most conservative option consists of considering equality between M_S and M_L. This option is used, for example, in the last revision of the French seismic zonation (Martin et al. 2002a). However, a more common judgement is that M_L is greater than M_S for earthquakes with magnitudes smaller than 6.0. Here, we adopt the relation proposed by Nicolas (2000), i.e. $M_S = 1.56 M_L - 3.31$. Within the logic tree, the following magnitude transformation procedures are adopted. For the relationships of Ambraseys (1995) and Ambraseys et al. (1996), two epistemic choices are considered: no magnitude conversion (i.e. $M_S = M_L$) and magnitude conversion using the relation of Nicolas (2000). Weights for the two options are not very different with a slight preference for the Nicolas (2000) option (0.52 and 0.48 for $M_S = M_L$).

4.5 Aleatory uncertainties

Parameters affected by aleatory uncertainties are the GR activity parameters λ and β, focal depth h and

Table 6 Coefficients of $\log_{10}(A) = C_1 + C_2 M_L + C_3 \log_{10} r + C_4 r \pm \sigma$ corresponding to the ground-motion prediction equations of Tapia et al. (2007) for PGA and SA and for a depth of 10 km

T(s) (h_0=10 km)	Freq (Hz)	$C_1(f)$	$C_2(f)$	C_3(Z)	$C_4(f)$	σ
0.0 (PGA)	34.00	0.6	0.41	−1.0	−0.0034	0.462
0.1	10.00	1.1	0.35	−1.0	−0.0033	0.438
0.3	3.33	−0.9	0.73	−1.0	−0.0023	0.457
0.6	1.67	−2.5	0.99	−1.0	−0.0015	0.532
1.0	1.00	−3.3	1.06	−1.0	−0.0011	0.576
2.0	0.50	−3.9	1.05	−1.0	−0.0004	0.577

Acceleration A is expressed in g.

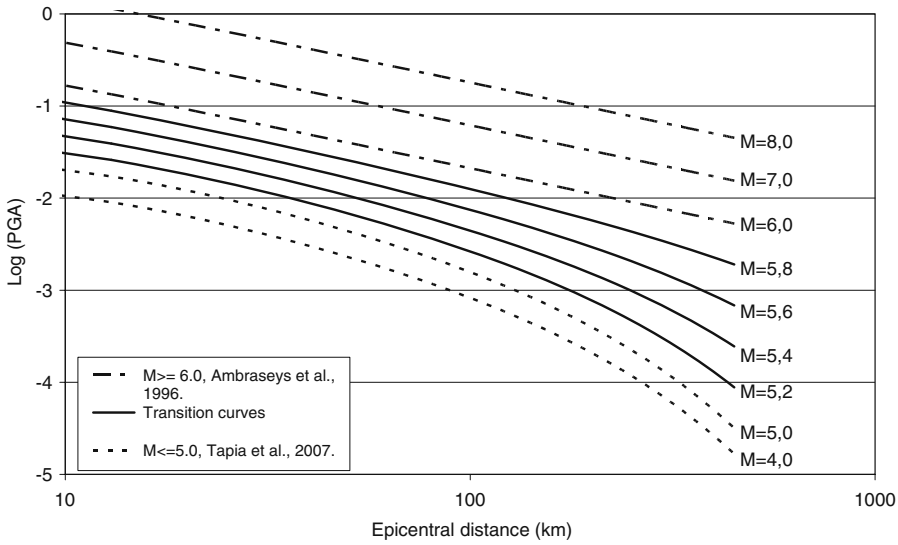

Fig. 9 Schema of the regional ground-motion prediction equation proposed for different magnitude values

maximal magnitude M_{max}. A Gaussian distribution is chosen for the GR parameters, while a uniform distribution is chosen for depth and maximum magnitude. The standard deviations of λ and β, h and M_{max} interval bounds are shown in Table 4 for the USZ model and Table 5 for CFZ.

Uncertainties associated with these parameters are propagated using a Monte Carlo approach coupled to the logic tree. Values of the four parameters are randomly selected inside the associated probability distribution for the hazard calculation. For each epistemic choice on the logic tree, this process is repeated 100 times.

For hazard assessment using the smoothing method of Woo (1996), aleatory uncertainties affect focal depth h and the R_{max} parameter of the kernel function. The probability distribution used for h assumes a probability 0.2 for h=5 km, 0.6 for h=10 km and 0.2 for h=15 km. R_{max} was assumed to follow a uniform distribution between 40 and 60 km.

4.6 Seismic hazard maps

The exceedance probability of an acceleration level at rock sites is calculated for PGA and for five structural periods: 0.1, 0.3, 0.6, 1 and 2 s. Calculation is performed at each point of a grid with a mesh size of 0.1°. Results from the logic tree and Monte Carlo simulation are treated to obtain at each point the median value of the acceleration and values for the 15% and 85% percentiles.

Seismic hazard is represented in terms of iso-acceleration maps for the 475- and 1,975-year return periods. PGA maps are illustrated in Figs. 11 and 12. Acceleration contour lines delineate two main areas

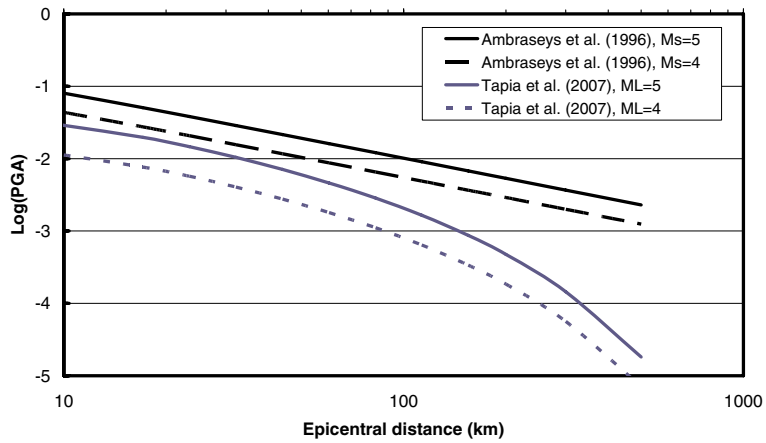

Fig. 10 Comparison between the PGA predicted by Ambraseys et al. (1996) and the relationship developed by Tapia et al. (2007)

for seismic hazard. The most active area is in the French part of the western Pyrenees. Contours are stretched along the mountain axis. Median PGA reaches a maximal value between 150 and 200 cm/s^2 for a 475-year return period. On the Spanish side, the 100–150 cm/s^2 level is reached near 1° W–43° N. PGA decreases to the south, and reaches 50 cm/s^2 near 42° N.

Another maximum is reached along the massif axis in the east part of the Pyrenees near 2.3° E (Fig. 11). However, in this area, maximum median PGA is lower, around 125 cm/s^2. This is also the acceleration level in the region of Andorra. Acceleration contour lines in the eastern Pyrenees delineate a more diffuse zone with median PGAs ranging from 100 to 125 cm/s^2, stretched along a north–south axis until Barcelona.

The hazard map for a return period of 1,975 years shows similar contours (Fig. 12). The acceleration levels for a 1,975-year return period are around 40% higher in the Central western Pyrenees than those for a 475-year return period. For the Catalonia region, this increase is up to 100%.

Similar maps have been produced for structural periods 0.1, 0.3, 0.6, 1 and 2 s. Uniform hazard response spectra can be estimated for each point on the hazard maps. Figure 13 shows examples of uniform hazard response spectra for four cities for a return period of 475 years. Uncertainties estimated using the logic tree and Monte Carlo approach are represented by 15th and 85th percentiles curves.

Finally, a map with the maximum accelerations probably felt during the past was constructed using the epicentral data of the new ISARD catalogue and by applying the Ambraseys (1995) ground-motion prediction equation to all earthquakes (Fig. 14). The magnitude transformation hypothesis considered is M_S=M_L. The focal depth adopted is 10 km for all earthquakes. This map shows the maximum acceleration obtained for each point of the rectangular grid used (resolution of 0.1°). This map shows equivalent or greater motions in the southern and eastern Pyrenees than in the western central Pyrenees region where the probabilistic 475-year hazard map gives higher accelerations. In the western Pyrenees, the 475-year hazard is dominated by moderate earthquakes with short occurrence times, while in the east and south, strong motions are mainly associated with great historical earthquakes with longer occurrence periods.

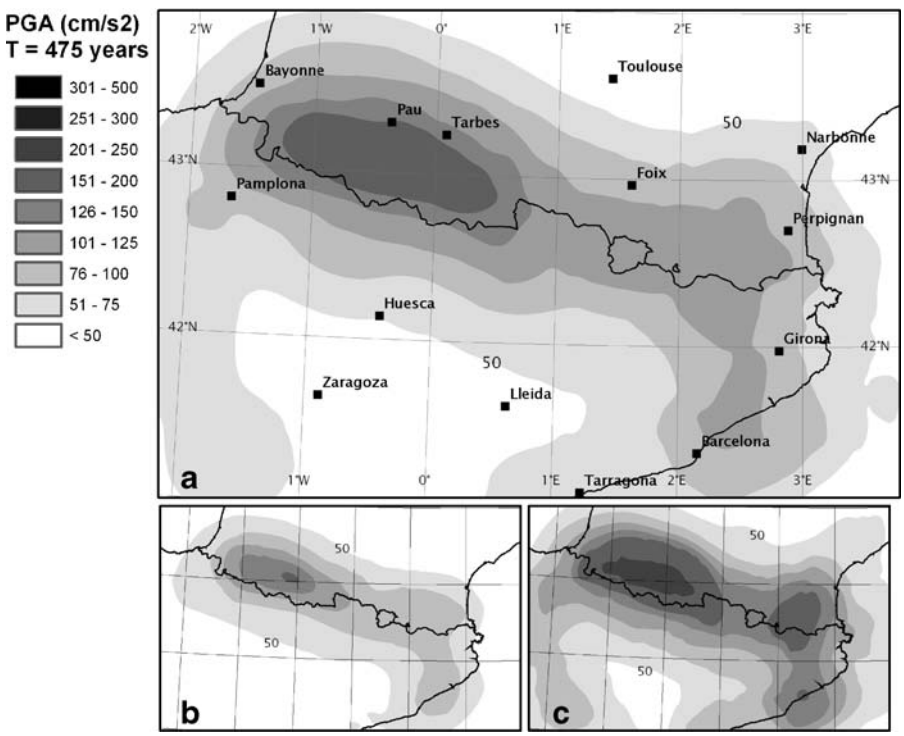

Fig. 11 Seismic hazard map for the Pyrenean region for PGA and 475-year return period. **a** Median; **b** 15th percentile, **c** 85th percentile

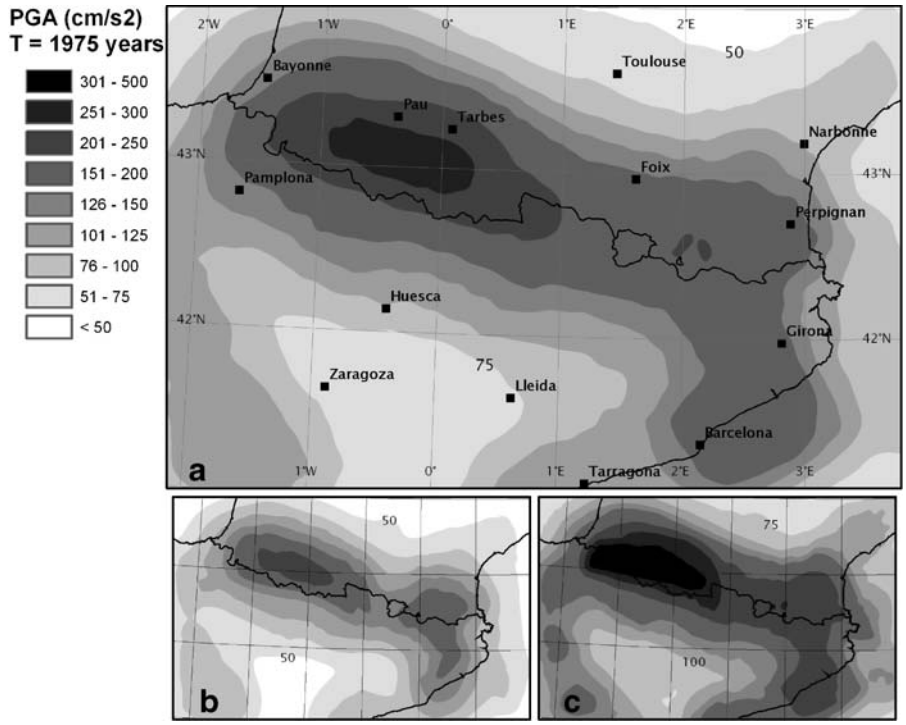

Fig. 12 Seismic hazard map of Pyrenean region for PGA and 1,975-year return period. **a** Median, **b** 15th percentile, **c** 85th percentile

5 Conclusions

A PSHA of the Pyrenean region has been performed using French and Spanish data. Historical and instrumental seismic catalogues from the two countries have been merged and analysed to build a single trans-border seismic catalogue, called ISARD. Local magnitude M_L is adopted as the reference magnitude scale because it is the most commonly used magnitude in the regional catalogues.

A combined Monte Carlo and logic tree analysis has been developed to take into account a selection of epistemic choices and random uncertainties.

In this region of low to moderate seismicity and where the current knowledge of seismic activity associated with active faults is poor, delimitation of source zones has a great influence on hazard assessment. To reduce this influence, a first epistemic choice is to consider two conceptual models for hazard calculation: zoning and non-zoning methodologies. The first one uses the PSHA software CRISIS99 (Ordaz et al. 1999) with a classical representation of seismic area sources. The non-zoning method is based on Woo (1996) and directly uses the epicentres from the ISARD catalogue to calculate the hazard. Another epistemic choice consists in selecting different seismogenic models: the USZ model resulting from a synthesis of several recent models and a consensus between experts and the CFZ model coming from a zoning currently used in France and merged with the USZ in the southern part of the study area.

Two ground-motion prediction models are considered. One (using Ambraseys (1995) for PGA and Ambraseys et al. (1996) for SA) is widely used in Europe for similar seismotectonic contexts. The other is a local ground-motion prediction equation. It is the first time that a PSHA of this region uses a ground-motion prediction equation derived from the available regional data. Special care has been taken in the selection of the magnitude definition to assure that the magnitudes of the catalogue are compatible with the magnitudes of the ground-motion prediction equations. For use with the ISARD catalogue, two M_S–M_L transformations are proposed: the Nicolas (2000) relationship and $M_S=M_L$.

The final results consists of seismic hazard maps expressed in terms of median values, 15th and 85th percentiles for SA (for 0 [PGA], 0.1, 0.3, 0.6, 1 and 2 s) and 475- and 1,975-year return periods. Finally, a map showing estimates of the historical accelerations

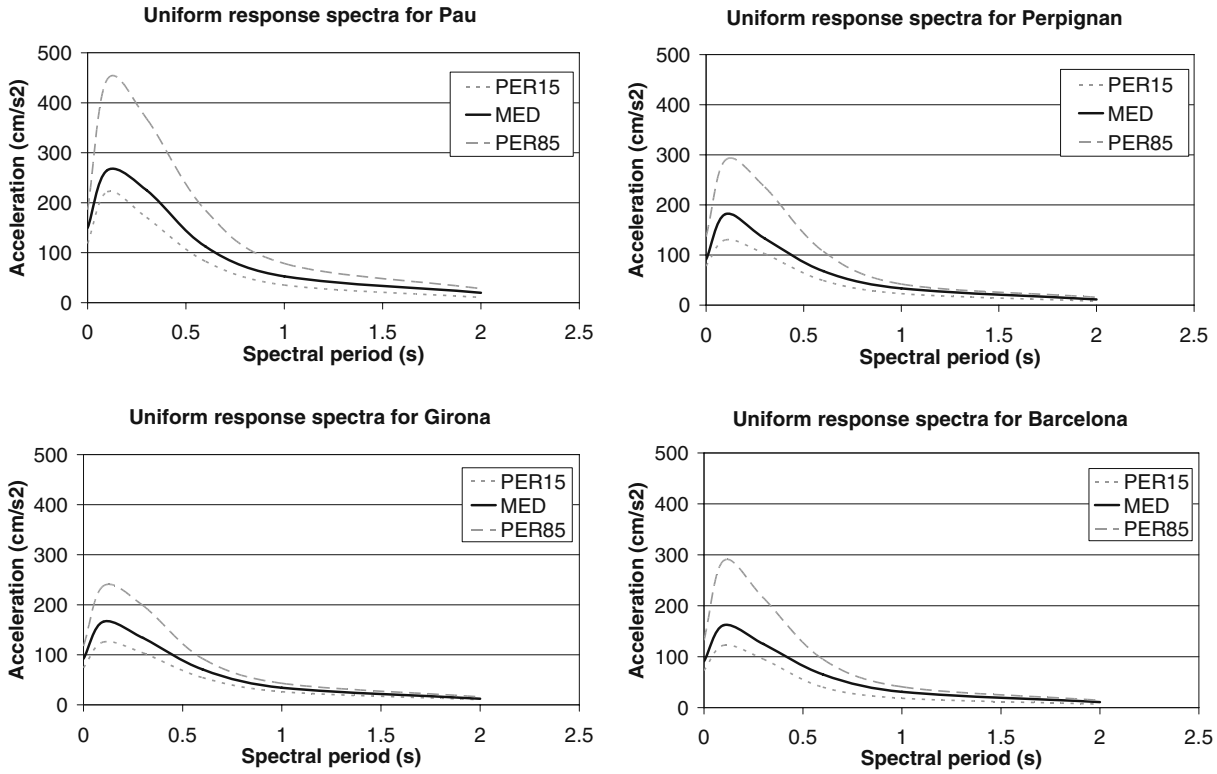

Fig. 13 Uniform hazard response spectra (median, 15th and 85th percentile) for the 475-year return period in: Barcelona (Spain), Girona (Spain), Perpignan (France) and Pau (France)

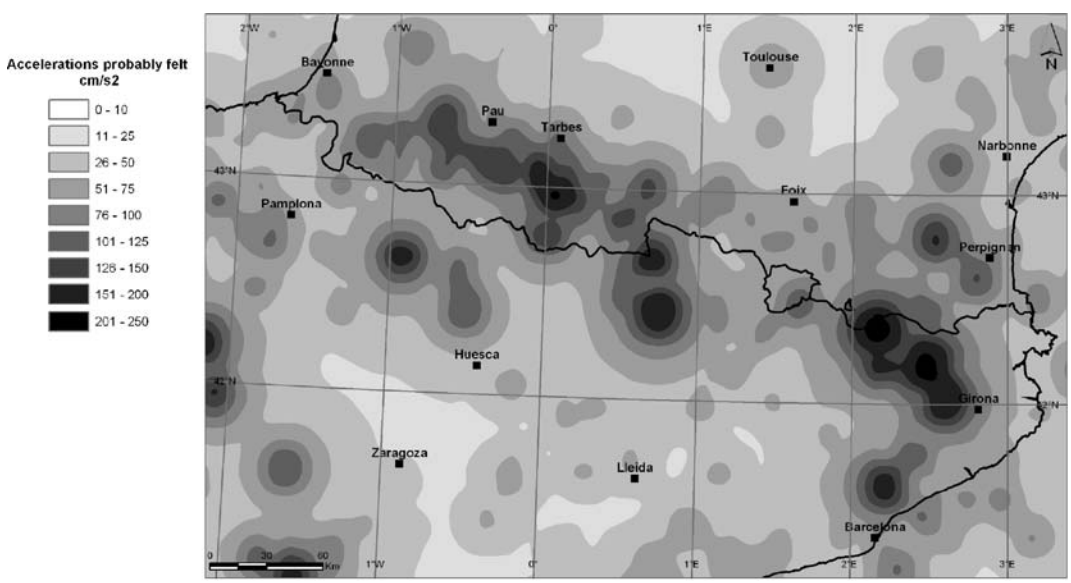

Fig. 14 Maximum acceleration probably felt in the region based in the ISARD catalogue and the Ambraseys (1995) ground-motion prediction equation

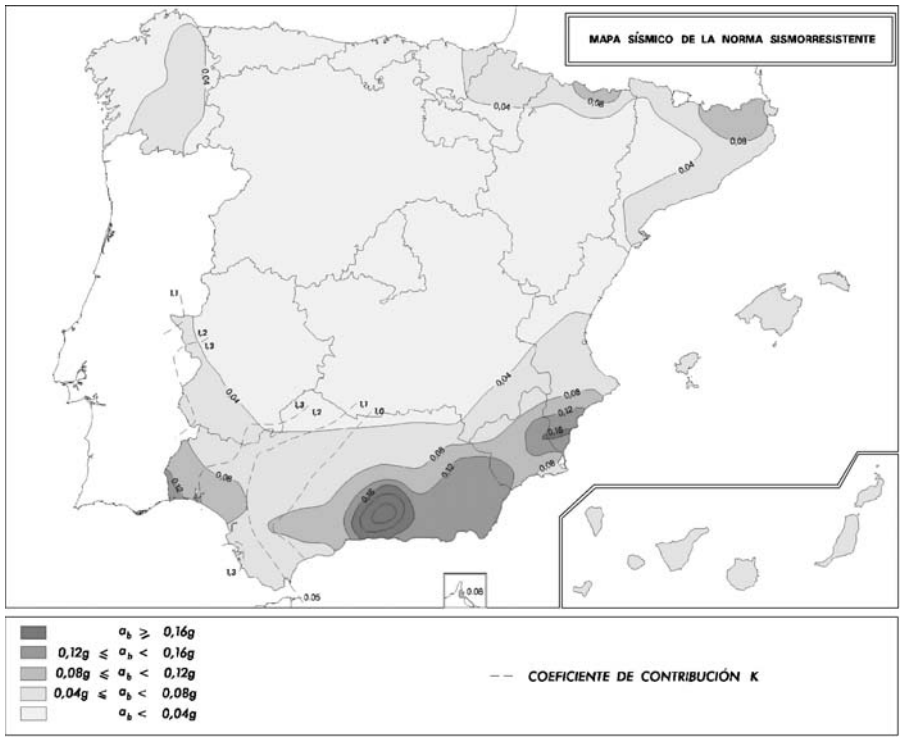

Fig. 15 Seismic zonation of Spain from the Spanish seismic design code (NCSE-02 2002)

probably registered during the period of the earthquake catalogue was produced.

A comparison between the present assessment and the acceleration levels proposed in recent seismic zonations for Spain and France demonstrates non-negligible differences. The official seismic zonation of Spain (NCSE-02 2002), expressed in terms of a_b corresponding to values of PGA associated to a 475-year return period, is presented in Fig. 15. For the border zone, it shows lower values of acceleration (0.04 to 0.12g) than the ISARD maps, especially in the western part where values higher than 0.15g are obtained here.

The latest revision of the seismic zonation for France (Martin et al. 2002a) shows higher acceleration levels

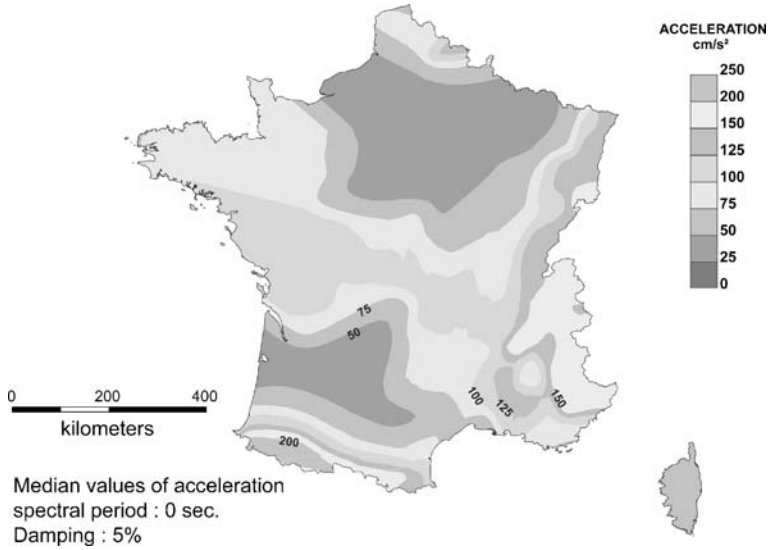

Fig. 16 Seismic zonation of France (Martin et al. 2002a, b) for the revision of French seismic design code

than the maps of the present study (Fig. 16). However, the shape of the iso-value curves is similar on the French side of the border. A global increase of 0.03*g* on the eastern part to 0.05*g* in the western part is observed. One of the main reasons for these differences could be the hypothesis $M_S=M_L$ made in the French seismic zonation. On this map, the acceleration contour lines are stretched along the axis of the massif. The two distinct activity zones seen on the ISARD maps, centred in the western Pyrenees and in Catalonia, do not appear in this French zonation.

The probabilistic approach to seismic hazard in Metropolitan France by Marin et al. (2004) shows much lower acceleration levels in Pyrenees than the present assessment. As example, the 475-year return period maximum PGA in the central Pyrenees is around 0.067*g*. in Marin et al. (2004), and it is roughly 0.2*g* in the present study. One reason is that a single zone is considered for all the Pyrenees in Marin et al. (2004). In a sensitivity study and with a division of this zone in five distinct areas, Marin et al. (2004) found that acceleration levels in the western central zone increase by a factor 2.5.

Therefore, the differences observed among different seismic zonations could be attributed to the input data used, the methodology of calculation and the hypotheses considered. The approach performed within the ISARD project tries to be a first step towards a necessary homogenisation of seismic hazard maps in Europe and, particularly, along the France–Spain border.

Acknowledgements This work was supported by the Interreg IIIA France Spain 2000–2006 programme. We thank J. Irizarry and J. Douglas for revising the English. We would like to thank two anonymous reviewers for the critical reviews and useful suggestions that really improved the manuscript.

References

Abrahamson NA (2000) State of the practice of seismic hazard evaluation. In: GeoEng Conference Proceedings, Melbourne, Australia, pp 659–685

Alasset PJ, Meghraoui M (2005) Active faulting in the western Pyrénées (France): paleoseismic evidence for late Holocene ruptures. Tectonophysics 409:39–54

Ambraseys NN (1995) The prediction of earthquake peak ground acceleration in Europe. Earthq Eng Struct Dyn 24:467–490

Ambraseys NN, Simpson KA, Bommer JJ (1996) Prediction of horizontal response spectra in Europe. Earthq Eng Struct Dyn 25:371–400

Autran A, Bles JL, Combes Ph, Cushing M, Dominique P, Durouchoux C, Mohammadioun B, Terrier M (1998) Probabilistic seismic hazard assessment in France, Part 1: seismotectonic zonation. In: ECEE'98, Paris

Blès JL, Bour M, Dominique P, Godefroy P, Martin C, Terrier M (1998) Zonage sismique de la France métropolitaine pour l'application des règles parasismiques aux installations classées. Documents BRGM, no. 279, 56 p

BRGM, EDF, IRSN (2004) SisFrance. Available at: http://www.sisfrance.net

Cornell CA (1968) Engineering seismic risk analysis. Bull Seismol Soc Am 58:1583–1606

Daignières M, De Cabissole B, Gallart J, Hirn A, Suriñach E, Torné M, ECORS Pyrénées Team (1989) Geophysical constraints on the deep structure along de ECORS Pyrénées line. Tectonics 8:1051–1058

Dominique P, Autran A, Bles JL, Fitzenz D, Samarcq F, Terrier M, Cushing M, Gariel JC, Mohammadioun B, Combes P, Durouchoux C (1998) Probabilistic seismic hazard assessment in France, Part 2: probabilistic approach: seismic hazard map on the national territory (France). In: Seismotectonic zonation, ECEE'98, Paris

Faccioli E (2006) Seismic hazard assessment for derivation of earthquake scenarios in Risk-UE. Bull Earthq Eng 4:341–364

Fleta J, Escuer J, Goula X, Olivera C, Combes P, Grellet B, Granier Th (1996) Zonación Tectónica, primer estadio de la zonación sismotectónica del NE de la Península Iberica (Catalunya). Tectonic zoning, firs stage of seismotectonic zoning of NE Iberian Peninsula (Catalonia). Geogaceta 20:853–856

Goula X, Olivera C, Fleta J, Grellet B, Lindo R, Rivera LA, Cisternas A, Carbon D (1999) Present and recent stress regime in the Eastern part of the Pyrénées. Tectonophysics 308:487–502

Jiménez M-J, García-Fernández M, the GSHAP Ibero-Maghreb Working Group (1999) Seismic hazard assessment in the Ibero-Maghreb region. Annali di Geofisica, GSHAP Special Volume

Levret A, Cushing M, Peyridieu G (1996) Recherche des caractéristiques de séismes historiques en France. Atlas de 140 cartes macrosismiques. IPSN, Paris, France (2 volumes)

Marin S, Avouac JP, Nicolas M, Schlupp A (2004) A probabilistic approach to seismic hazard in metropolitan France. Bull Seism Soc Am 94(6):2137–2163

Martin C, Combes P, Secanell R, Lignon G, Firavanti A, Carbon D, Monge O, Grellet B (2002a) Revision du zonage sismique de la France. Etude probabiliste. Rapport GEOTER GTR/MATE/0701-150

Martin C, Secanell R, Lignon G (2002b) Automation of the seismic hazard calculation by means of probabilistic approaches. Preliminary results in France. In: Proc. III asamblea Hispano-Portuguesa de Geodesia y Geofísica, Valencia, 2002

Martinez-Solares JM, Mezcua J (2002) Catálogo Sísmico de la Península Ibérica (800 A.C.–1900). Instituto Geográfico Nacional, monografía no. 18, Madrid

Mezcua J, Martinez-Solares JM (1983) Sismicidad del Área Ibero-Mogrebí, pub 203. Instituto Geográfico Nacional, Madrid

McGuire R (1976) EQRISK. Evaluation of earthquake risk to site. Fortran computer program for seismic risk analysis. US Geological Survey. Open File. Report 76-67 (92 pp)

NCSE-02 (2002) Norma de construcción sismoresistente. BOE no. 244. Viernes 11 Octubre 2002

Nicolas M (2000) Relation entre magnitude M_S et M_L (LDG) pour les séismes localisés en France métropolitaine V1.0. Rapport CEA/DIF/DASE/LDG/ DO 145 (9 pp)

Nocquet JM (2002) Mesure de la déformation crustale en Europe occidentale par géodésie spatiale. PhD thesis, Université de Nice, Sophia Antipolis (311pp)

Olivet JL (1996) La cinématique de la plaque ibérique Elf Aquitaine production. Bull Cent Rech Explor Prod Elf Aquitaine 20:131–195

Ordaz M, Aguilar A, Arboleda J (1999) Program for computing seismic hazard, CRISIS99-18 Ver.1.018. UNAM University, Mexico

Secanell R, Goula X, Susagna T, Fleta J, Roca A (1999) Mapa de zonas sísmicas de Cataluña. In: 1er Congreso Nacional de Ingeniería Sísmica, Múrcia, pp 251–259

Secanell R, Irizarry J, Martin C, Susagna T, Goula X, Combes P, Fleta J (2002) Unified probabilistic seismic hazard assessment around the France-Spain border. In: Proc. XXVII General Assembly European Seismological Commission, Genoa

Secanell R, Goula X, Susagna T, Fleta J, Roca A (2004) Seismic hazard zonation of Catalonia, Spain, integrating random uncertainties. J Seismol 8:25–40

SGC (2003) Servei Geològic de Catalunya. SGC, Catalonia, Spain (Computer file)

Souriau A, Pauchet H (1998) A new synthesis of Pyrenean seismicity and its tectonic implications. Tectonophysics 290:221–244

Stepp JC (1972) Analysis of completeness of the earthquake sample in the Puget Sound area and its effect on statistical estimates of earthquake hazard. In: Proceedings the 2nd International Conference on Microzonation, pp 897–910

Susagna T, Goula X (1999) Catàleg de sismicitat. Atlas sísmic de Catalunya, vol. 1. Institut Cartogràfic de Catalunya, Catalonia, Spain (436 pp)

Talaya J, Feigl K, Termens A, Colomina I (1999) Practical lessons from analysis of a GPS network design to protect movements or ~1 mm/year in the eastern Pyrenees. Phys Chem Earth A 24(4):355–359

Tapia M, Susagna T, Goula X, Irizarry J (2004) Ley de atenuación del suelo en el noreste de España. In: 4ª Asamblea Hispano Portuguesa de Geodesia y Geofísica

Tapia M, Susagna T, Goula X (2007) Curvas predictivas del movimiento del suelo en el oeste del Mediterráneo. In: 3er Congreso Nacional de Ingeniería Sísmica, 8–11 Mayo 2007, Girona, 17pp

Terrier M, Bles JL, Godefroy P, Dominique P, Bour M, Martin C (2000) Zonation of Metropolitan France for the application of earthquake-resistant building regulations to critical facilities. Part 1: seismotectonic zonation. J Seismol 4:215–230

Verges J (1993) Estudi geològic del vessant sud del Pirineu oriental i central: evolució cinemàtica en 3D. PhD thesis, University of Barcelona, Spain (203 pp.)

Weichert DH (1980) Estimation of the earthquake recurrence parameters for unequal observational periods for different magnitudes. Bull Seismol Soc Am 70:1337–1346

Woo G (1996) Kernel estimation methods for seismic hazard area source modelling. Bull Seismol Soc Am 86(2):353–362